Silicon carbide nanostructures: A tight binding approach

Anthony D. Patrick,[1,2] Xiao Dong,[1] Thomas C. Allison,[3] and Estela Blaisten-Barojas[1,2,a)]
[1]*Computational Materials Science Center, George Mason University, 4400 University Dr. MSN 6A2, Fairfax, Virginia 22030, USA*
[2]*Department of Computational and Data Sciences, George Mason University, 4400 University Dr. MSN 6A2, Fairfax, Virginia 22030, USA*
[3]*National Institute of Standards and Technology, 100 Bureau Drive, Stop 8320, Gaithersburg, Maryland 20899, USA*

(Received 6 March 2009; accepted 2 June 2009; published online 23 June 2009)

A tight-binding model Hamiltonian is newly parametrized for silicon carbide based on fits to a database of energy points calculated within the density functional theory approach of the electronic energy surfaces of nanoclusters and the total energy of bulk 3C and 2H polytypes at different densities. This TB model includes *s* and *p* angular momentum symmetries with nonorthogonal atomic basis functions. With the aid of the new TB model, minima of silicon carbide cagelike clusters, nanotubes, ring-shaped ribbons, and nanowires are predicted. Energetics, structure, growth sequences, and stability patterns are reported for the nanoclusters and nanotubes. The band structure of SiC nanotubes and nanowires indicates that the band gap of the nanotubes ranges from 0.57 to 2.38 eV depending on the chirality, demonstrating that these nanotubes are semiconductors or insulators. One type of nanowire is metallic, another type is semiconductor, and the rest are insulators. © *2009 American Institute of Physics*. [DOI: 10.1063/1.3157282]

I. INTRODUCTION

Elemental and molecular clusters in the nanoscale size regime are of interest because of their potential use in nanodevices. Studies of hollow clusters such as fullerenes unveiled their unusual physical properties, which find use in a multitude of applications.[1] For example, these structures can be used as conducting nanobridges between two nanoelectrodes,[2] or as nanocarriers for delivering molecules from one part of a system to another.[3] Silicon carbide is the only chemical compound of carbon and silicon. Silicon carbide nanoclusters possess unique properties compared to bulk materials, due to quantum size effects, high thermal conductivity, high electric field breakdown strength, and maximum heat exchange. These properties make SiC a promising candidate for high-powered nanodevices.

The exploration for the existence of elemental fullerene-like and nanotube structures other than carbon gained much attention in recent years.[4–10] Theoretical predictions dismissed silicon as a candidate for fullerene and nanotube growth because this element preferentially selects sp^3 bonding instead of the characteristic sp^2. Because the silicon-carbon bond is stronger than the silicon-silicon bond, an approach for stabilizing silicon sp^2 bonded structures is to dope it with carbon. Recently Sun *et al.*[11] reported the synthesis of silicon carbide nanotubes and nanowires produced via the reaction of Si with carbon nanotubes. In view of the fact that SiC nanotubes have been synthesized successfully, a large family of SiC cages is expected to exist similar to the fullerenes. Several groups found techniques for growing SiC nanowires[12–14] and these nanostructures are expected to expand uses of this strong material in nanoversions of thermistors (temperature variable resistors) and varistors (voltage variable resistors).

Theoretical studies of SiC nanostructures are scarce and tend to be based on a variety of methodologies.[15–17] In this study a tight-binding (TB) model[18,19] was adapted for use in nanosystems by fitting the relevant parameters to a set of small elemental clusters. Recently, we put forward a successful fitting strategy of this TB model for monoatomic elemental clusters.[20–22] In this paper we apply this fitting strategy in the context of a binary compound and demonstrate its portability for nanostructures. The methodology relies on a parametrization of the TB Hamiltonian that incorporates structural and energetic knowledge of small SiC clusters. To that extent, a database of energies associated with the electronic energy surface of several small SiC clusters was built, with all electron calculations done at the density functional theory (DFT) approach. The TB model developed allows then for study of a multitude of nanosystems. Throughout this study the ratio of Si to C is one-to-one, which ensures the same stoichiometry than in all SiC bulk polytypes. Other TB models could have been considered for this study. However, the selection of the TB of Refs. 18 and 19 is based on the extensive computational infrastructure that we developed by having used it in the past. This paper is organized as follows. Section II gives a description of the TB parametrization and includes the energetics of the small SiC clusters used in its development. Sections III–V give the specifics of energies, structure, growth sequences, and band structure of nanocages, nanotubes, and nanowires. Section VI concludes this work.

a)Electronic mail: blaisten@gmu.edu.

II. THE TIGHT-BINDING MODEL FOR SIC

The TB scheme is a rough quantum approach that permits studies of systems involving 10^2-10^3 atoms in a unit cell at a reasonable computational expense. Recently we parametrized a TB model[18,19] for calcium clusters including *s*, *p*, and *d* atomic-like nonorthogonal orbitals and used it extensively.[20–22] In the case of a binary system such as SiC we consider only *s*, *p* atomic-like nonorthogonal orbitals. This TB model follows the Slater–Koster approach,[23] which is an extension of Bloch's linear combination of atomic orbitals method,[24] in which the *i*th atom in a unit cell has a set of atomic-like orbitals associated with it. The main characteristic of this TB model is giving an analytical description to the Hamiltonian and overlap matrix elements. The analytical expressions representing the matrix elements contain parameters that are further fitted to theoretical calculations or empirical data. These integrals are referred to as on-site, hopping, and overlap.

The on-site integrals are given in terms of the local atomic density. For a two component system, each atom *i* belongs to one of two atom types, Si or C in our case. Then the local atomic density at the *i*th site contributed by atoms of a given type is

$$\rho_{i_\nu} = \sum_j e^{(-\lambda_\nu^2 R_{ij})} F(R_{ij}), \tag{1}$$

where ν is either Si or C, j enumerates atoms of type ν, R_{ij} are the distances between atoms, λ_ν is a parameter, and $F(R)$ is a cutoff function, which in this study is defined as follows:

$$F_c(R) = \frac{\Theta(12.5-R)}{1+e^{2(R-12.5)}}, \tag{2}$$

with interatomic distances R given in Bohr. For SiC there are two parameters λ_C and λ_{Si}. The analytical representation of the on-site integrals at the *i*th site includes contributions from two atom types:

$$O_{l\nu} = \alpha_{l\nu} + \sum_{\nu'} [\beta_{l\nu\nu'}\rho_{\nu'}^{2/3} + \gamma_{l\nu\nu'}\rho_{\nu'}^{4/3} + \epsilon_{l\nu\nu'}\rho_{\nu'}^{2}], \tag{3}$$

where l is either an *s* or *p* orbital, ν' is either Si or C, $\alpha, \beta, \gamma, \epsilon$ are parameters, and $\rho_{\nu'}$ is the local atomic density of type ν'. Therefore, for SiC, there are four α parameters and 24 β, γ, ϵ parameters.

The hopping integrals taking into account *s* and *p* orbitals for SiC are $ss\sigma$, $sp\sigma$, $pp\sigma$, $pp\pi$, and $ps\sigma$. The latter is only considered for dissimilar atom types. These integrals are represented by a product of a polynomial and an exponential that depends on the local environment of atoms,

$$H_{ll'm}(R) = (a_{ll'm} + b_{ll'm}R + c_{ll'm}R^2)e^{(-d_{ll'm}^2 R)}F_c(R), \tag{4}$$

where a, b, c, d are parameters, l, l' are subindices identifying the orbitals, and m identifies the integral type. There are 52 parameters entering in the hopping integrals for SiC. The overlap integrals have the same functional representation as the hopping integrals for SiC, but for Si and C a different functional form is adopted,

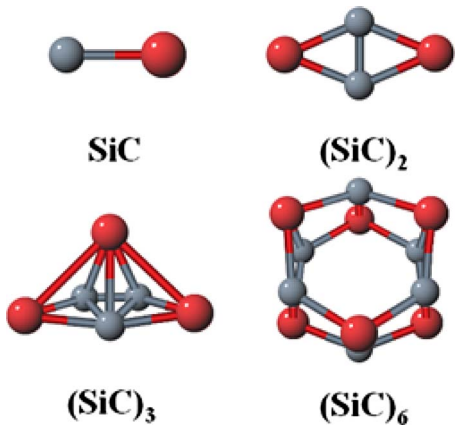

FIG. 1. (Color online) Optimized SiC clusters used in the fit of the TB parameters.

$$O_{ll'm}(R) = (\delta_{ll'} + a_{ll'm}R + b_{ll'm}R^2 + c_{ll'm}R^3)e^{(-d_{ll'm}^2 R)}F_c(R), \tag{5}$$

where the first term is a Kronecker delta function. The overlap integrals contain 52 parameters, which completes a total of 134 parameters entering Eqs. (1)–(5).

The strategy in this work is to fit the 134 parameters to a set of energies calculated within the DFT formalism. The Levenberg–Marquardt algorithm (LMA) is used to optimize the fit. With this purpose, given a set of independent energy points (target), one calculates a set of energies from the TB model corresponding to the same configurations used to obtain the target energies. The TB-calculated energies depend on the 134 model parameters. The LMA optimizes the parameters such that the sum of the squares of the deviations between target and TB-calculated energies becomes minimal. Thus, the LMA is an iterative procedure that finds minima of the deviation-squares-sum in parameter space. This method has a robust performance in the optimization of models containing many parameters. We applied this methodology for fitting the parameters of a range of classical model potentials to target points obtained with quantum chemical approaches.[20,25–27] In these past studies, as well as in this work, the central component of the strategy is to have a comprehensive database of target points that contains electronic energies of both small clusters and extended bulk solids. The expectation is that the model parameters fitted on this size-diverse energy points will reproduce important quantum finite size properties while retaining an acceptable description of bulk properties.

The database of target energies for fitting the 134 TB parameters contains crystal data and cluster data. For the cluster data, the database includes 37 points of SiC, $(SiC)_2$, $(SiC)_3$, and $(SiC)_6$ electronic energy surfaces calculated within all-electron DFT, the Becke three-parameter functional, and nonlocal corrections.[28] The GAUSSIAN 2003 package,[29] B3LYP functional, and 6-311G basis set were employed to calculate these 37 target energies included in the database. Optimized structures of these clusters are shown in Fig. 1 and their binding energies at the minimum, symmetry, electronic state identification, and average SiC bond length

TABLE I. Symmetry, ground state, binding energy of SiC clusters calculated with DFT used in the fitting process, and comparison to TB energies.

	DFT			TB fit			
SiC_n	Sym	State	E_b/n (eV)	E_b/n (eV)	E_b^{relaxed}/n (eV)	Error/n (eV)	No. points
SiC	$C_{\infty v}$	$^1\Sigma_g$	−3.0558	−3.5876	−3.8812	0.04	9
$(SiC)_2$	D_{2h}	^1A_g	−8.1730	−6.7462	−7.0751	0.12	9
$(SiC)_3$	C_s	$^1A'$	−8.5136	−7.7626		0.07	9
$(SiC)_6$	C_i	^1A_g	−8.2310	−7.8070	−8.1100	0.04	9
$(SiC)_{12}$	T_h	^1A_g	−9.4573	−9.2161	−9.4677		

are reported in Table I. The cluster electronic states are singlets and the reported binding energies are relative to the energy of the separated Si and C in their triplet states. The 37 points on the electronic energy surface of these clusters were produced by homogeneously stretching and compressing each cluster. For the crystal data, the total energy and the energy bands of two SiC crystalline polytypes were included. Eleven configurations of the 3C polytype (cubic) with different densities consistent with lattice constant a ranging from 4.18 to 4.34 Å, plus 22 configurations of the SiC 2H polytype (hexagonal) with densities consistent with a ranging from 3.02 to 3.09 Å and lattice constant ratio $c/a=1.64$ were considered. Eight energy bands (85 k-points each) were considered for the 3C crystal and 16 energy bands (76 k-points each) were included for the 2H polytype. Energies of these 33 crystals and their corresponding energy bands were calculated with the published TB parameters,[17] which are based on DFT results of these crystals.

Because the calculated bulk energies contain an arbitrary energy shift and the calculated cluster energies are actual binding energies, both energies need to be relative to a consistent reference of energies. The adopted criterion for establishing the value of the energy shift was to make the 3C polytype equilibrium energy coincide with the experimental cohesive energy of −12.68 eV. This introduces the 135th parameter to the TB model, which is a shift of 0.340 272 Ry/SiC that is to be applied to all energies calculated with our new TB parametrization.

The optimal 135 parameters are reported in Table II. These TB parameters enter Eqs. (1)–(5) and are used throughout this work for the nanostructures studied in the next sections. Use of these parameters yields energies in Ry and distances in Bohr. Table I contains a comparison of the cluster relaxed energies using the new TB parameters as compared with the TB energies at the geometry of the DFT calculation used as a target in the fit. To test the portability of the new model, the optimized DFT-calculated binding energy of $(SiC)_{12}$ was obtained and the corresponding TB-calculated energy compared to it. Table I shows this comparison and also shows that as the cluster is relaxed under the TB the agreement with DFT results improve. Note that energy points of $(SiC)_{12}$ were not included in the database of target points on which the TB model was fitted.

III. SIC CAGES

TB model parametrizations are not universal. It is then important to understand how the model performs for nanostructures with different surface structures. For example, the published parameters of the SiC TB model[17] work well for the crystalline polytypes but do not give rise to stable nanostructures.[30] Cagelike clusters have been studied at the DFT level for many sizes.[31] However, there has been no attempt to generate those cages with a simpler model such as the TB. We find it then interesting to demonstrate that the new TB model parametrization is suitable for cage nanostructures. To achieve this objective a variety of SiC cage-clusters were formed by constraining all bonds to be Si–C. Such construction originates ring formations containing even number of SiC, which are referred to as *members* of the ring. Bulk polytypes contain even-member rings indicating that Si–Si bonds and C–C bonds would only occur at imperfections. In this study four-membered rings (4MRs) and six-membered rings (6MRs) are considered for building hollow cages following the rules set forward in Ref. 31. For cages with n SiC consisting of 4MRs and 6MRs, the number of 4MRs is always equal to six, whereas the number of 6MRs is $n-4$. This mathematical relationship remains true for any polyhedron containing only 4MRs and 6MRs. Thus, with increasing cluster size, the number of 6MRs increases while the number of 4MRs remains constant. For example, both $(SiC)_9$ and $(SiC)_{11}$ have six 4MRs, whereas $(SiC)_9$ has five 6MRs and $(SiC)_{11}$ has seven 6MRs.

Fullerenelike $(SiC)_n$ with $n=6-28$, 36 cage structures were designed and further relaxed to yield the stable clusters illustrated in Fig. 2. Each reported structure corresponds to a minimum of the TB energy obtained with the Broyden–Fletcher–Goldfarb–Shanno algorithm.[32–35] Binding energies, symmetry, and average bond lengths for these cage clusters are reported in Table III. The cage energies are plotted in Fig. 3(a). The $(SiC)_{12}$ cage is remarkably stable and displays 4MRs with bond length of 1.85 Å and 6MRs with a slightly shorter bond length of 1.84 Å. For testing, the $(SiC)_{12}$ cage was optimized within DFT and the TB energy of the optimized $(SiC)_{12}$ is in agreement with the DFT optimized structure exhibiting a discrepancy of only 0.01 eV (see Table I). The bond lengths of the optimized TB $(SiC)_{12}$ are in agreement with those calculated with DFT for the 4MRs. However, the DFT optimization yields 6MRs bond lengths of 1.77 Å, which are shorter than the TB predictions. A previous DFT study of $(SiC)_n$ with smaller basis set[15] reported structures consistent with our TB results as seen in the comparison included in Table III. While the TB energies of $(SiC)_6$, $(SiC)_{16}$, and $(SiC)_{25}$ show discrepancies of up to

TABLE II. Optimized TB parameters entering in Eqs. (1)–(5) and Δ_{shift}=0.340 272 Ry.

	Si-on-site λ=−1.0741				C on Si			
	α	β	γ	ϵ	β	γ	ϵ	
s	0.1808	−5.7550	9.4253	58.5233	−3.0424	103.5573	1575.0681	
p	0.2535	−0.4857	21.4112	−45.2443	0.3707	10.7977	182.0098	
	C-on-site λ=−1.3778				Si on C			
s	−0.2242	10.0942	−204.3441	1292.2073	0.1454	2.4665	−12.7755	
p	0.3520	4.3943	−20.6489	225.2908	−0.0709	−2.831	1.9509	
	Si-hopping				Si-overlap			
	a	*b*	*c*	*d*	*a*	*b*	*c*	*d*
$ss\sigma$	6034.4143	−1135.8639	−434.8381	1.5322	−526.0569	152.6001	55.3983	1.4578
$sp\sigma$	18.9294	−3.9331	−0.9981	1.0387	123.6153	−56.5049	11.9368	1.2267
$pp\sigma$	−1.3296	−1.1699	0.5520	0.9134	8.3393	8.7567	−1.7924	1.0524
$pp\pi$	87.4304	18.1717	11.5249	1.4267	−21.2473	9.0960	−0.5759	1.0142
	C-hopping				C-overlap			
$ss\sigma$	1256.1372	−153.0547	−185.3339	1.6375	−8.5885	5.5014	−1.7288	1.3431
$sp\sigma$	−28.5564	8.9921	7.4110	1.3302	2.4803	−5.1381	0.8146	1.1372
$pp\sigma$	−24.7549	−0.2422	3.9502	1.1782	−3.4416	−0.2442	0.2462	1.0406
$pp\pi$	248.9705	−69.7619	−40.5988	1.5822	3.4676	−0.5051	0.0770	1.0283
	SiC-hopping				SiC-overlap			
$ss\sigma$	181.1326	3.8307	−28.2102	1.3512	21.1266	6.0707	−0.1465	1.2319
$sp\sigma$	0.5768	−1.5736	0.2062	0.8193	66 419.5435	−41 077.3644	6449.2913	1.6371
$ps\sigma$	−12.0911	5.7585	−0.4689	−0.8418	49.7669	8.9258	−12.8545	1.3148
$pp\sigma$	−8.5326	1.4151	0.5209	0.9664	17.7721	−6.6701	0.9366	0.9874
$pp\pi$	−0.8569	0.2356	−0.0174	0.4953	−50.1551	25.1366	−2.4331	1.0156

0.25 eV, the TB energy of the other structures is in remarkable good agreement with Ref. 15. The discrepancy in the case of $(SiC)_{16}$ (a D_{2d} structure) is possibly due to the loss of symmetry of the TB relaxed cluster when compared with the T_d previously reported DFT calculation performed with symmetry constraints. The overall dimension of this cage is about 5.88 Å and the Si–C bond lengths are 1.84 Å in the 4MRs and 1.83 Å in the 6MRs, which are close to the published results of 6.1 Å (cage size) and 1.804, 1.791 Å (bond lengths). The largest cagelike clusters $(SiC)_{27}$, $E_b^{relaxed}/n$, and C_i are new structures. Symmetry reduction occurs for $(SiC)_{36}$, since this cage could have been a T_d structure but relaxed to a D_{2d} under the TB model. As seen in Fig. 3(a), the binding energy per SiC decreases monotonically with the increase in the number of SiC molecules with the exception of some cluster sizes. The second difference of the binding energies, shown in Fig. 3(b), displays the relative stability of the clusters to the increase in one SiC. Peaks in this plot indicate clusters that are more stable than their neighboring sizes. The $(SiC)_{12}$ cluster has the largest second difference of the binding energy indicating that this cluster is a magic cluster among $(SiC)_n$ structures. The second difference of the binding energy was compared to Ref. 15 with good agreement in the smaller sizes and discrepancies as the cluster size is increased. This is probably due to the small structural changes of the clusters when relaxed under the TB model.

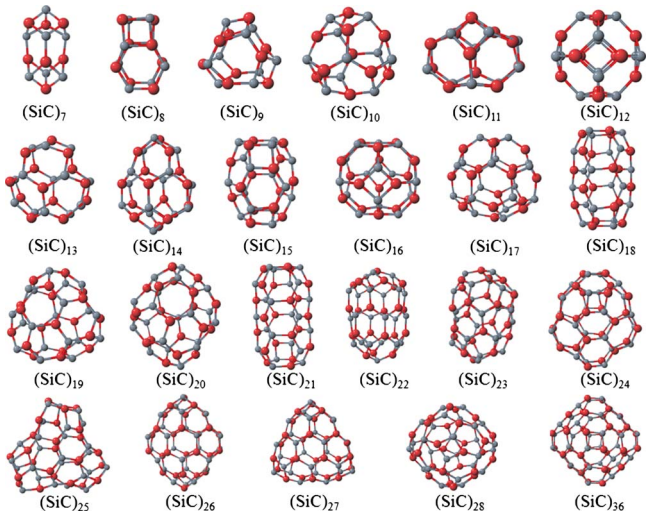

FIG. 2. (Color online) Structure of the SiC_n cagelike clusters optimized with the TB model. Carbon and silicon are depicted by light gray and dark gray (red) spheres, respectively.

IV. SIC TUBES AND RIBBONS

Several single-wall nanotubes consisting of Si and C with a 1:1 ratio are new to the literature and reported in this

TABLE III. TB binding energy of cagelike clusters and average bond length of the 4MR and 6MR.

SiC_n	Sym	No. of 6MR	4MR/6MR bond length (Å)	TB E_b/n (eV)	(Ref. 15) E_b/n (eV)
6	C_{2h}	2	1.87/1.76	−8.362	−8.122
7	C_{3v}	3	1.89/1.93	−8.225	−8.261
8	C_2	4	1.91/1.86	−8.703	−8.712
9	C_s	5	1.85/1.86	−8.928	−8.976
10	C_3	6	1.85/1.85	−9.032	−8.976
11	C_s	7	1.84/1.88	−9.248	−9.211
12	T_h	8	1.85/1.84	−9.469	−9.483
13	C_{3v}	9	1.89/1.84	−9.342	−9.345
14	C_s	10	1.85/1.85	−9.512	−9.488
15	C_{3h}	11	1.85/1.85	−9.632	−9.657
16	D_{2d}	12	1.84/1.85	−9.632	−9.748
17	C_s	13	1.84/1.85	−9.721	−9.692
18	C_3	14	1.85/1.85	−9.785	−9.770
19	C_3	15	1.84/1.88	−9.794	−9.753
20	C_1	16	1.83/1.86	−9.801	−9.796
21	C_{3h}	17	1.84/1.85	−9.876	−9.852
22	C_3	18	1.84/1.85	−9.881	−9.904
23	C_1	19	1.84/1.88	−9.935	−9.908
24	C_1	20	1.83/1.88	−9.893	−9.952
25	C_3	21	1.86/1.86	−9.814	−9.991
26	C_{2h}	22	1.83/1.85	−10.006	−9.996
27	C_{3v}	23	1.84/1.85	−10.040	
28	D_2	24	1.82/1.85	−10.067	
36	D_{2d}	32	1.83/1.86	−10.179	

section. Periodic boundary conditions were used to simulate infinite tubes, with the unit cell typically containing four layers of atoms in the direction of the length of the tube. Each tube is identified by the chiral vector notation (m,n) introduced for carbon nanotubes.[36] Two types of SiC tubes are studied: zigzag $(m,0)$ and armchair $(m/2,m/2)$ with $m=4$, 6, 8, 10, 12, 14, 16, and 20. Figure 4 shows cross sections of the smaller tubes with $m=4$, 6, 8, and 12 and a side view of the tube surface with different chirality. The armchair tubes are to the right of Fig. 4 and the zigzag tubes to the left. Calculated properties are included in Table IV. The band structure is composed of 16 band, each of them with 21 k-points. The TB calculation shows that the zigzag $(m,0)$ nanotubes are more stable than the armchair $(m/2,m/2)$ nanotubes, in agreement with past studies[37,38] and in contrast with the behavior of carbon nanotubes that display armchair nanotubes more stable than the zigzag counterpart.[39]

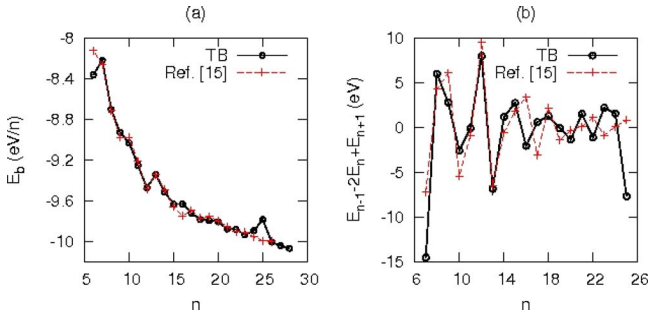

FIG. 3. (Color online) Energetics of the SiC cagelike clusters. (a) Binding energy per SiC as a function of cluster size. (b) Second difference of the binding energy. This work (dots). Reference 15 (crosses).

Table IV contains results for tubes with radius larger than 8 Å, which are new to the literature. The radius dependence of the band gap energy for zigzag and armchair SiC nanotubes is included in Table IV. It can be seen that as the radius of the tube increases the band gap increases until reaching a plateau. The zigzag SiC nanotubes have a direct band gap at the Γ-point, while the armchair tubes have an indirect band gap. The trends of our results are in agreement with DFT studies[38] with the TB band gaps being systematically larger as expected.

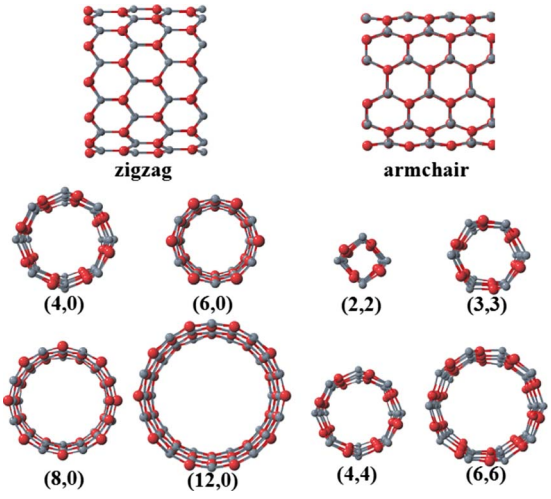

FIG. 4. (Color online) Single-wall SiC nanotubes identified by the chiral vector notation (m,n). The top illustrates the surface of the armchair (right) and zigzag (left) tubes. The bottom illustrates axial views. Carbon and silicon are depicted by light gray and dark gray (red) spheres.

TABLE IV. TB binding energies, band gap, and radius of SiC nanotubes with chirality $(m,0)$ and $(m/2,m/2)$.

	$(m,0)$			$(m/2,m/2)$		
m	R (Å)	E_b (eV/n)	Gap (eV)	R (Å)	E_b (eV/n)	Gap (eV)
4	2.03	−10.611	0.568	1.79	−10.010	1.827
6	3.03	−11.118	1.179	2.35	−10.360	2.185
8	4.02	−11.249	1.857	3.50	−10.472	2.283
10	5.02	−11.286	2.292	4.34	−10.534	2.256
12	6.03	−11.297	2.219	5.23	−10.569	2.192
14	7.05	−11.306	2.208	6.09	−10.590	2.139
16	8.02	−11.310	2.175	6.97	−10.604	2.187
18	9.05	−11.313	2.227	7.83	−10.613	2.148
20	10.02	−11.315	2.161	8.52	−10.620	2.118

The Si–C bond lengths are in agreement with Ref. 37, predicting Si–C bond lengths of 1.87 Å for both zigzag and armchair SiC nanotubes. On the other hand, DFT calculations predict a shorter Si–C bond length of 1.80 Å.[37,38] The Si–C bond length of the bulk 3C crystal is 1.89 Å. In this study bulk 3C–SiC was used in the development of the TB parameters, which could explain why the TB model tends to give long Si–C bond lengths. Relaxation of the atomic positions under the TB yields the Si atoms positioning themselves closer to the center of the tube with the C atoms positioning toward the outside. The surface reconstruction due to the slight difference in hybridization of Si and C atoms favors the most electronegative C atoms to be pushed outward while the Si atoms move inward shielding themselves from attack by nucleophiles. As the tube radius increases, the difference in radial position of Si and C becomes less noticeable.

In order to investigate the stability of the ring-shaped cross section of the tubes, the periodic boundary conditions were removed and ring shaped ribbon structures containing four layers of atoms were analyzed. These newly studied ringlike ribbons are clusters containing only 6MRs before relaxation. Once relaxed under the TB the structures notoriously tend to close up by forming an imperfect cage-looking cluster that contains only 6MRs. This behavior is quite strong in the ring shaped ribbonlike structure having chirality (3,3). Therefore, new ribbon-ring looking stable isomers of $(SiC)_{16}$ and D_{2d} are predicted, as well as other new ring shaped ribbon-type clusters as reported in Table V. Among these new clusters, the armchair $(SiC)_{24}$ is more stable than the cagelike isomer reported in Table III. Contrary to the nanotubes, the armchair ribbon structures are more stable than the zigzag ribbon structures. Surface reconstruction is apparent in these ribbonlike ring shaped structures similar to that occurring in the tubes.

TABLE V. TB binding energies of SiC_n ringlike clusters. Index m is the chirality of the ribbon before structural optimization.

		$(m,0)$	$(m/2,m/2)$
$(SiC)_n$	m	E_b (eV/n)	E_b (eV/n)
16	4	−9.206	−9.516
24	6	−9.510	−9.955
32	8	−9.579	−9.755
40	10	−9.612	−9.790
48	12	−9.621	−9.807

V. SIC NANOWIRES

Several SiC nanowires built from carved sections of the 2H and 3C polytype crystals are stable under the TB method. Figure 5 illustrates the cross section of four SiC wires. In all cases, the wires are periodic along the direction pointing out from the figure, which is in the direction of the face identified by the Miller indices of the bulk structure. The length of wires built from the 2H polytype are perpendicular to the [001] and [110] planes and wires built from the 3C polytope are perpendicular to the $[\bar{1}00]$ and $[\bar{1}11]$ planes. The band structure has 16 bands, each with 21 k-points. Each of these wires was relaxed within the TB model indicating that modest reconstruction of their surface takes place once the structure geometry is optimized.

The most stable wire is the 3C $[\bar{1}00]$ nanostructure depicted in Fig. 5 with a binding energy of −11.7 eV/SiC. The next most stable wire is the 2H [001] with binding energy of −11.6 eV/SiC. The 3C $[\bar{1}11]$ wire is next in stability with a

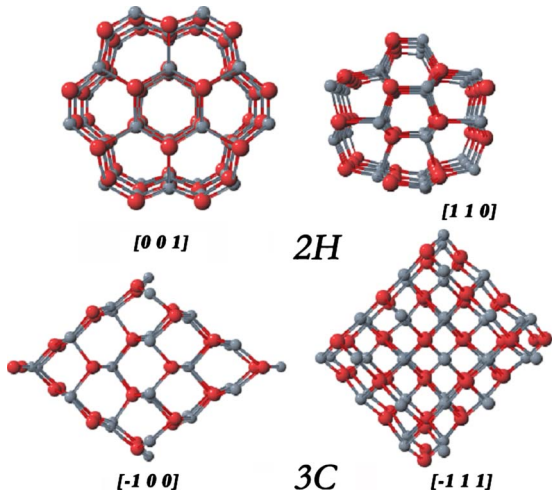

FIG. 5. (Color online) Cross section of nanowires obtained from cuts of the 2H and 3C crystal polytypes. Carbon and silicon are depicted by light gray and dark gray (red) spheres.

binding energy of −11.0 eV/SiC and the most unstable wire is the 2H [110] with a binding energy of −10.3 eV/SiC. Stability preference predicts then the most probable growth direction of a specific SiC polytype nanowire. Analysis of the band structure of the four wires indicates that the 2H [001] wire presents a 2.1 eV band gap, the largest of all of the wires studied, clearly indicating that this type of wire is an insulator. On the other hand, the least stable 2H [110] wire is metallic, the 3C $[\bar{1}00]$ wire has a small band gap of 0.4 eV and could be considered to be a semiconductor. The 3C $[\bar{1}11]$ wire is also a semiconductor with a band gap of less than one eV.

VI. CONCLUSION

A new TB model is developed and used to predict structural properties of SiC nanostructures including cagelike clusters, ring-shaped ribbons, nanotubes, and nanowires. This TB model has 135 parameters and works well for clusters that have carbon atoms bonded with silicon atoms in a one-to-one composition ratio. Results for the smaller cages are in agreement with previous DFT findings[15] and the TB-optimized nanotubes with smaller radius are in agreement with previous TB and DFT studies.[37,38] Thus, we are very confident that the novel cages, nanoribbon clusters, nanotubes, and nanowires are possible nanostructures that are yet to be obtained experimentally. Numerous large SiC nanoclusters with cage and ribbon structures are predicted to be stable. The predicted (4,0), (6,0) nanotubes and the 3C $[\bar{1}11]$, 3C $[\bar{1}00]$ nanowires are semiconductors, the 2H [110] nanowire is metallic, and all other nanotubes and nanowires studied here are insulators.

ACKNOWLEDGMENTS

This work was partially supported by the National Institute of Standards and Technology. Teragrid Grant No. PHY050023T is acknowledged for computing time. We acknowledge useful discussions with Dr. Carlos Gonzalez and Dr. D. Papaconstantopoulos.

[1] A. K. Ray and M. N. Huda, J. Comput. Theor. Nanosci. **3**, 315 (2006).
[2] A. W. Ghosh and S. Datta, J. Comput. Electron. **1**, 515 (2002).
[3] Y. Shirai, A. J. Osgood, Y. Zhao, K. F. Kelly, and J. M. Tour, Nano Lett. **5**, 2330 (2005).
[4] M. Cote, M. L. Cohen, and D. J. Chadi, Phys. Rev. B **58**, R4277 (1998).
[5] D. L. Strout, J. Phys. Chem. A **104**, 3364 (2000).
[6] S. S. Alexandre, M. S. C. Mazzoni, and H. Chacham, Appl. Phys. Lett. **75**, 61 (1999).
[7] N. G. Chopra, R. J. Luyren, K. Cherry, V. H. Crespi, M. L. Cohen, S. G. Louis, and A. Zettl, Science **269**, 966 (1995).
[8] R. Tenne, L. Margulis, M. Genut, and G. Hodes, Nature (London) **360**, 444 (1992).
[9] Y. Feldman, E. Wasserman, D. J. Srolovitz, and R. Tenne, Science **267**, 222 (1995).
[10] J. Pattanayak, T. Kar, and S. Scheiner, J. Phys. Chem. A **106**, 2970 (2002).
[11] X. H. Sun, C. P. Li, W. K. Wong, N. B. Wong, C. S. Lee, S. T. Lee, and B. K. Teo, J. Am. Chem. Soc. **124**, 14464 (2002).
[12] H. J. Dai, E. W. Wong, Y. Z. Lu, S. S. Fan, and C. M. Lieber, Nature (London) **375**, 769 (1995).
[13] Z. Pan, H. L. Lai, F. C. K. Au, X. F. Duan, W. Y. Zhou, W. S. Shi, N. Wang, C. S. Lee, N. B. Wang, S. T. Lee, and S. S. Xie, Adv. Mater. (Weinheim, Ger.) **12**, 1186 (2000).
[14] S. G. Sundaresan, A. V. Davydov, M. D. Vaudin, I. Levin, J. E. Maslar, Y. L. Tian, and M. V. Rao, Chem. Mater. **19**, 5531 (2007).
[15] R. Wang, D. Zhang, and C. Liu, Chem. Phys. Lett. **411**, 333 (2005).
[16] P. Erhart and K. Albe, Phys. Rev. B **71**, 035211 (2005).
[17] N. Bernstein, H. J. Gotsis, D. A. Papaconstantopoulos, and M. J. Mehl, Phys. Rev. B **71**, 075203 (2005).
[18] M. J. Mehl and D. A. Papaconstantopoulos, Phys. Rev. B **54**, 4519 (1996).
[19] D. A. Papaconstantopoulos and M. J. Mehl, J. Phys.: Condens. Matter **15**, R413 (2003).
[20] X. Dong, G. M. Wang, and E. Blaisten-Barojas, Phys. Rev. B **70**, 205409 (2004).
[21] X. Dong and E. Blaisten-Barojas, J. Comput. Theor. Nanosci. **3**, 118 (2006).
[22] X. Dong, S. Gatica, and E. Blaisten-Barojas, Comput. Lett. **1**, 152 (2005).
[23] J. C. Slater and G. F. Koster, Phys. Rev. **94**, 1498 (1954).
[24] F. Bloch, Z. Phys. **52**, 555 (1928).
[25] E. Blaisten-Barojas and S. N. Khanna, Phys. Rev. Lett. **61**, 1477 (1988).
[26] C. H. Chien, E. Blaisten-Barojas, and M. R. Pederson, J. Chem. Phys. **112**, 2301 (2000).
[27] G. M. Wang, E. Blaisten-Barojas, A. E. Roitberg, and T. P. Martin, J. Chem. Phys. **115**, 3640 (2001).
[28] A. D. Becke, J. Chem. Phys. **98**, 5648 (1993).
[29] M. J. Frisch, G. W. Trucks, H. B. Schelgel *et al.*, GAUSSIAN 03, Gaussian Inc., Pittsburgh, PA, 2003.
[30] A. Patrick, Ph.D. dissertation, George Mason University, December 2008.
[31] H. S. Wu, F. Q. Zhanq, X. H. Xu, C. J. Zhang, and H. Jiao, J. Phys. Chem. A **107**, 204 (2003).
[32] C. G. Broyden, J. Inst. Math. Appl. **6**, 222 (1970).
[33] R. Fletcher, Comput. J. **13**, 317 (1970).
[34] D. GoldFarb, Math. Comput. **24**, 23 (1970).
[35] D. F. Shanno, Math. Comput. **24**, 647 (1970).
[36] J. W. Mintmire, B. I. Dunlap, and C. T. White, Phys. Rev. Lett. **68**, 631 (1992).
[37] M. Menon, R Richter, A. Mavrandonakis, G. Foudakis, and A. N. Andriotis, Phys. Rev. B **69**, 115322 (2004).
[38] M. Zhao, Y. Xia, F. Li, R. Q. Zhang, and S. T. Lee, Phys. Rev. B **71**, 085312 (2005).
[39] D. H. Oh and Y. H. Lee, Phys. Rev. B **58**, 7407 (1998).